Computational Materials Science 93 (2014) 137–143

Contents lists available at ScienceDirect

Computational Materials Science

journal homepage: www.elsevier.com/locate/commatsci

Direct quantification of solute effects on grain boundary motion by atomistic simulations

Hao Sun, Chuang Deng *

Department of Mechanical Engineering, University of Manitoba, Winnipeg, MB R3T 5V6, Canada

ARTICLE INFO

Article history:
Received 1 April 2014
Received in revised form 6 June 2014
Accepted 24 June 2014

Keywords:
Segregation
Solute drag
Grain boundary motion

ABSTRACT

Direct quantification of grain boundary mobility with the presence of impurities poses a great challenge for investigating thermal stability of nanocrystalline alloys. By applying the interface random-walk method, we investigate the dopant segregation and precipitation from direct molecular dynamics simulations. It is found that existing atomistic simulation methods based on pure grain boundaries can be readily extended to extract the mobility of impure grain boundaries. Furthermore, it is confirmed that the grain boundary motion is controlled by the diffusion of segregated dopants at the interface as assumed by many theoretical models, but the grain boundary mobility is directly related to the impurity diffusion in the direction perpendicular to the boundary plane. By directly quantifying the mobility of impure grain boundary under experimental conditions, a correction to the well-accepted solute drag model is proposed.

1. Introduction

Nanocrystalline materials are generally unstable and suffer from rapid grain growth when exposed to high temperatures [1–5], which poses great challenge to maintain their superior properties over their coarse-grained counterparts during thermal processing or service. In recent years, many controlled experiments [1,6], analytical modeling [6,7], and atomistic simulations [8,9] have suggested alloying as an effective approach to stabilize grain boundary (GB) networks through the segregation of selected alloying elements at GBs. In particular, a regular solution model originally proposed by Cahn, Lücke and Stüwe (referred as CLS model) [10–12] has been widely used to study the solute drag effects on migrating GBs; it is assumed in the CLS model that the GB migration is controlled by the diffusion of segregated dopant atoms that move along with the migrating interface. However, although experimental studies on the mobility of GBs containing impurities have been made in the past [2], those studies have been mainly limited to extremely low concentrations, e.g., less than 10 ppm [2]. A direct quantification of the GB mobility with the presence of dopants over several orders of magnitude from either experiments or simulations, which is the key input to validate the CLS model, is still missing.

With the rapid development of high performance computation, various methods based on molecular dynamics (MD) have been developed to extract GB mobility [13–17]. Nevertheless, almost all past simulations were limited to pure systems; only a few qualitative studies have been done on the stabilization of GB networks in nanocrystalline materials by addition of impurities. For example, Millett et al. [8,9,18] have studied bulk nanocrystalline Cu with impurities segregated in the GB regions to investigate their influences on grain growth during annealing at constant temperature of 800 K. The GB energy was found to decrease with the increase of the impurity concentration and the atom radius mismatch between impurity and bulk atom. However, a quantitative prediction between the GB mobility and impurity concentration was not established. One main reason is that most MD methods require unrealistically high driving forces to enable atom transfer across the boundary so that the overall GB migration can be detected in typical MD time scale [13–16]. On the other hand, the rate of boundary migration in impure systems is mainly determined by the diffusional process of the impurities [10–12,19–21], which is too slow to be studied by MD. In addition, the simulation cell must be large enough to form a steady-state impurity profile normal to the GB plane [20]. However, such limitations in MD may be overcome by using the interface-random-walk (IRWalk) method [17,22,23], which is capable of extracting GB mobilities based on purely thermal fluctuations according to:

$$D_{GB} = \frac{d\langle \vec{d}^2 \rangle}{t} \sim \frac{2MkT}{A} \quad (1)$$

* Corresponding author.
E-mail address: dengc@ad.umanitoba.ca (C. Deng).

http://dx.doi.org/10.1016/j.commatsci.2014.06.040
0927-0256/

where D_{GB} is the "diffusion" coefficient of the GB plane, T is temperature, A is the interface area, M is the GB mobility. To date, however, this method has been only applied to study pure GBs.

IRWalk method has been successfully applied in various pure GB systems to extract mobilities that were consistent with those extracted based on the driven motion methods at the low driving force limit in the past [17,23,24]. However, no attempt has been made yet to extend IRWalk method to investigate GBs containing impurities. The purpose of this work is thus to extend the IRWalk method to impure systems and directly quantify the mobilities of impure GBs under experimental conditions. It is also hoped to quantitatively validate the CLS model and fill the gap between MD simulations and analytical modeling in the past.

2. Methodology

2.1. MD simulation geometry and procedure

An inclined Σ5 GB in three types of Al-based alloys was simulated by MD using LAMMPS [25] with embedded-atom method potentials including Al–Ni [26], Al–Pb [27], and Al–Ti [28] with time step of 5 fs. The misorientation angle of the GB is 53.16° and the lattice orientations of the two grains are shown in Fig. 1(a). Various concentrations of impurity atoms, e.g., 2, 5, 10, 20, 41, 61 Ni, Pb, or Ti atoms, were introduced into the model by randomly replacing Al atoms at the GB region prior to the simulations, which correspond to 0.1%, 0.25%, 0.5%, 2.05%, 3.05% coverage of the GB by impurity atoms respectively. The initial simulation cell was set to be 5.69 nm × 5.69 nm × 10.48 nm in x, y and z directions (Fig. 1), respectively, accommodating 20,608 atoms. The geometry of this simulation cell is similar to the reference case proposed by Mendelev et al. for studying GB motions [24]. Periodic boundary conditions were applied along the x and y directions while the two surfaces perpendicular to the z-axis were free. Isothermal–isobaric ensemble (NPT) was used for the first 100 ps to relax the model and canonical ensemble (NVT) was used afterwards for all simulations. It needs to be mentioned that although the relaxation method used in this study may not be able to result in the physically equilibrated structure of the GBs, the interface random walk behavior of the GBs due to thermal fluctuation should not be significantly influenced [22,23]. For each alloy system of a specific concentration, 20 simulations (different random velocity initialization) up to 10 ns were performed. Atomic configurations of each alloy system were visualized by AtomEye [29]. The GB position can be determined by using an order parameter which depends on the local lattice orientation [22,23]. The system temperature was kept at 850 K so that significant GB fluctuation can be observed in these alloys. It has been tested at this temperature that a time step of 5 fs can well maintain the energy conservation in an NVE (micro-canonical ensemble) simulation, which ensures that the time step of 5 fs used in this study will speed up the simulation while maintaining the same degree of accuracy as compared to simulations with shorter time step such as 1 or 2 fs.

2.2. Determination of GB mobility by IRWalk method

According to the interface-random-walk method which was originally proposed by Trautt et al. [17], the GB mobility is correlated to the variance of GB displacements among a large number of independent simulations as described by Eq. (1). For each of

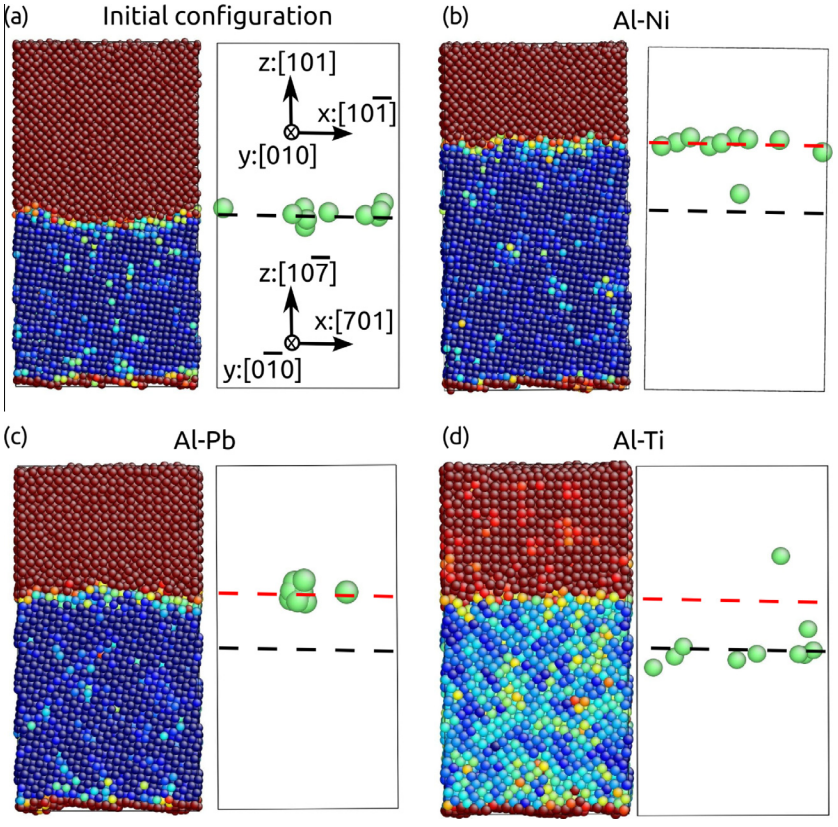

Fig. 1. (a) The initial atomistic configurations of the simulation cell in Al–Ni. The current atomistic configurations of the simulation cell during the GB thermal fluctuation are in (b) Al–Ni, (c) Al–Pb, and (d) Al–Ti. On the left the atom color corresponds to an order parameter depending on the local lattice orientation and on the right only dopant atoms are shown. The black and red dashed lines mark the initial and current GB positions, respectively. (For interpretation of the references to color in this figure legend, the reader is referred to the web version of this article.)

the 20 simulations of 10 ns duration, we recorded the GB position every 5 ps. In order to extract the GB mobility M, the displacement $d(i)$ after $5i$ ps was calculated based on the GB position $p(i)$ according to $d(i) = p_i((l+1)i) - p_j(li), (l = 0.1, \ldots, \left[\frac{2000}{i}\right],\ j = 1, 2 \ldots 20,\ i = 1, 2 \ldots 2000)$. With this adaptation, an equivalent of $20 \times \left[\frac{2000}{i}\right]$ independent data points can be obtained for GB displacement $d(i)$ during $t = 5i$. Accordingly, the variance of GB displacement $\langle \bar{d}^2(i) \rangle$ during time $t = 5i$ can be calculated as:

$$\langle \bar{d}^2(i) \rangle = \frac{1}{20\left[\frac{2000}{i}\right]} \sum_{i=0}^{\left[\frac{2000}{i}\right]} (p_i((l+1)i) - p_j(li))^2 \quad (2)$$

Since the GB fluctuation was strong at the temperature that we studied here (850 K for Al), no other adaptation or statistical enhancement is needed to process the data.

3. Results and discussion

3.1. Impurity segregation and precipitation from direct MD simulations

As shown in Fig. 1(a), the dopant atoms were initially placed at the GB region. Here the atom color on the left corresponds to an order parameter that depends on the local lattice orientation [13,22,23]; the Al atoms on the right were removed to show dopant atoms only. Depending on the alloy system, the dopant atoms behaved dramatically different as the GB fluctuated and moved away from its original position. Representative results were shown in Fig. 1(b–d) for systems containing 10 Ni, Pb, and Ti dopant atoms respectively with the black and red dashed lines marking the initial and current average GB positions. It is found that Ni atoms moved along with the GB which indicated strong segregation (Fig. 1(b)), Pb atoms aggregated and formed a precipitation which also moved along with the GB (Fig. 1(c)), whereas Ti atoms were left behind the migrating GB and almost stayed at their original positions. As a result, the following discussion will focus on Al–Ni and Al–Pb only. It is worth mentioning that in all these systems the GB has moved a substantial distance away from its initial position.

While GB segregation and precipitation has been commonly observed in experiments [7] and studied by both analytical modeling [7] and Monte Carlo simulations [30,31], it is encouraging to observe clear solute segregation and precipitation by direct MD simulations. In order to confirm that the GB segregation and precipitation shown in Fig. 1 was not transitional, we compared the evolution of the average GB position with the center-of-mass (COM) of the dopant atoms of different solute concentrations in both Al–Ni and Al–Pb alloy systems; one example is shown in Fig. 2(a and b) for Al–Ni with 2 and 40 Ni atoms respectively. It can be seen that in both cases, the evolution of the COM of Ni atoms and the average GB position almost overlapped each other for up to 10 ns. Moreover, the evolution of GB displacement up to 10 ns among 20 independent simulations in Al–Ni alloy system with 2 and 40 Ni atoms was shown in Fig. 2(c and d). It is found that solute segregation would not affect the random walk behavior of the GB during thermal fluctuation and the higher the dopant concentration, the smaller the variance of GB fluctuation.

3.2. GB mobility extracted from IRWalk method

Since it is confirmed in Fig. 2(c and d) that the thermal fluctuations of GBs that contain segregated or precipitated impurity atoms still exhibited random walk behavior, we can now extend the IRWalk method to extract the mobility of impure GBs. The representative results were shown in Fig. 3. In Fig. 3(a and b), the evolution of the variance of GB displacement with time was plotted for different dopant concentrations in Al–Ni and Al–Pb, which consistently showed a linear trend as predicted by Eq. (1). The GB mobility at various dopant concentrations in both Al–Ni and Al–Pb was then extracted according to Eq. (1) and plotted in Fig. 3(c); it is clearly shown that the GB mobility decreased as the number of dopant atoms increased in both systems. This trend is in excellent agreement with past experimental studies [2], analytical modeling [7,20,21,31], and indirect MD simulations [32]. For

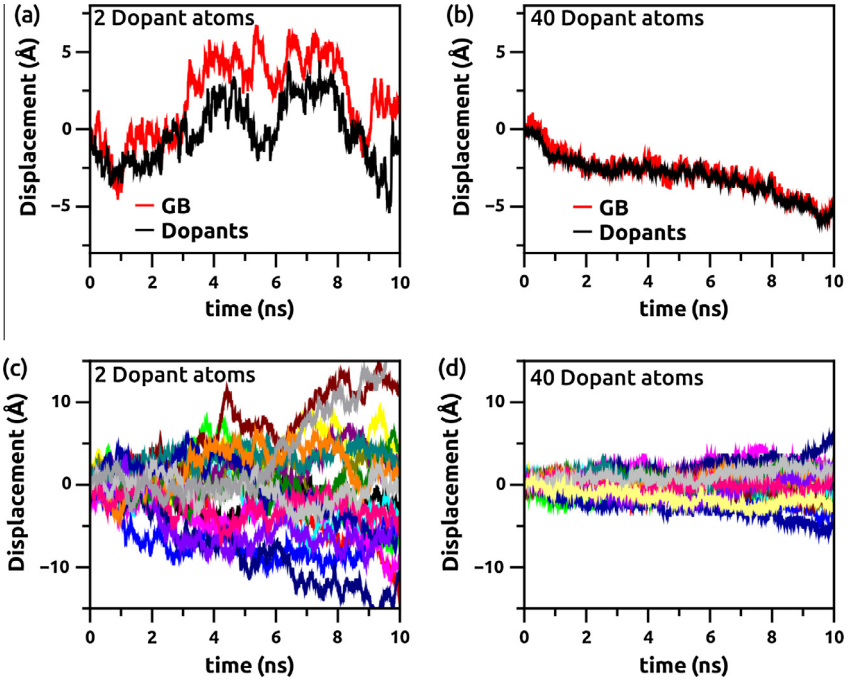

Fig. 2. Evolution of the displacement of GB and the center-of-mass of dopant atoms in Al–Ni system with (a) 2 and (b) 40 Ni atoms. Evolution of the average GB displacement in Al–Ni containing (c) 2 and (d) 40 Ni atoms based on 20 independent simulations.

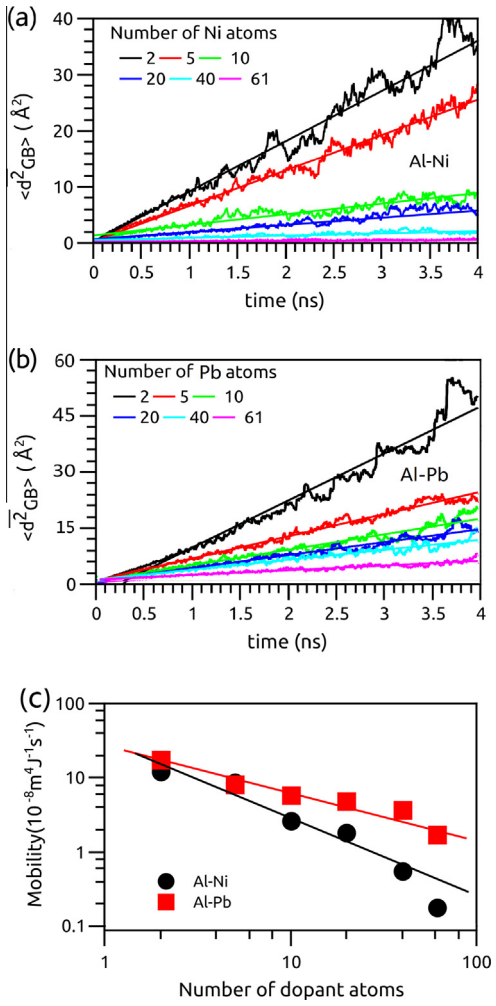

Fig. 3. (a) The evolution of the variance of average GB displacement in Al–Ni. (b) The evolution of the variance of average GB displacement in Al–Pb. (c) GB mobility as a function of the number of dopant atoms in both Al–Ni and Al–Pb.

example, Mendelev and Srolovitz [20,31] have predicted that the GB mobility would reversely proportional to the bulk concentration for the case of attraction of impurities to the boundary based on the CLS model. Mendelev and Srolovitz [32] have also used MD simulations to parameterize the CLS model in Al–Fe system and confirmed this trend.

On the other hand, it is interesting to find out that Ni atoms can stabilize the GB more effectively than Pb. While one possible reason is because of the different potentials that have been used for Al–Ni and Al–Pb systems, the dramatically different behaviors of Ni and Pb atoms during the GB fluctuation may have played a more important role than the atomic size. According to the phase diagram of Al–Pb system, Pb has extremely low solid solubility in Al and melts at the temperature used in the simulations (850 K). Therefore, Pb atoms would aggregate and form a second phase particle, which is consistent with that shown in Fig. 1(c). A large number of Pb atoms would thus occupy the bulk lattice sites instead of the sites within the GB region. In contrast, Al–Ni at all concentrations considered in this study can form a uniform solid solution at 850 K. As shown in Fig. 1(b), the Ni atoms distributed broadly in the GB area and most of them occupied the sites within the GB plane. Consequently, Ni atoms were more efficient than Pb in covering the GB area and lowering the GB mobility in Al-based alloy systems.

3.3. Comparison between GB mobility extracted from IRWalk and driven motion method

In order to validate that the IRWalk method can indeed be extended to extract physical mobility of GBs containing impurities, we also extracted the mobility of the same Al–Ni GB with 10 Ni atoms in the GB area by the so-called artificial driving force method [13,23,24] based on $V = MP$, where V is the GB velocity due to an applied driving force P, and M is the GB mobility. Here we applied a relatively small driving force of $P = 0.98$ MPa to ensure that the linear relationship between GB velocity and the applied driving force is not significantly deviated [23] and that the dopant atoms can catch up with the moving GB. As shown in Fig. 4(a), the impurity (Ni) atoms could move along with the GB under the applied driving force, which means that the segregation behavior was independent of the simulation methods. The GB displacement from 20 independent simulations for the same GB but with different initial conditions was plotted in Fig. 4(b), which shows similar random walk behavior as in Fig. 2(a). However, the average displacement among the 20 simulations due to the applied driving force showed an linear increase with time, as plotted in

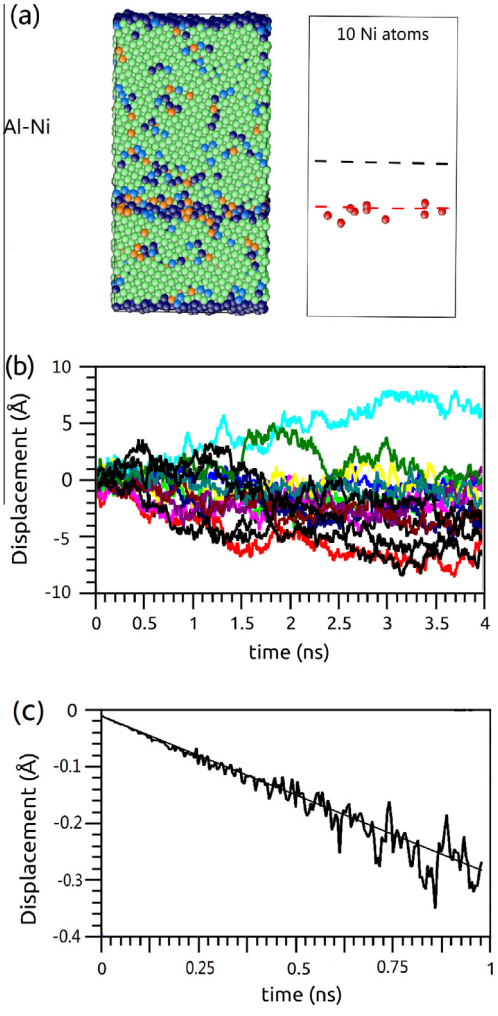

Fig. 4. (a) The representative initial and current atomistic configurations of the simulation cell during the GB thermal fluctuation in Al–Ni with an applied driving force of $P = 0.98$ MPa. On the left the atom color corresponds to the local lattice orientation and on the right only dopant atoms are shown. The black and red dashed lines mark the initial and current GB positions, respectively. Evolution of the (b) individual and (c) average GB displacement in Al–Ni containing 10 Ni atoms with driving force of $P = 0.98$ MPa among 20 independent simulations. (For interpretation of the references to color in this figure legend, the reader is referred to the web version of this article.)

Fig. 4(c), the slope of which is the GB velocity ($V = -0.026$ m/s). The mobility for Al–Ni system with 10 Ni atoms in GB based on this method is thus calculated to be $2.70 \times 10^{-8}\,m^4\,J^{-1}\,s^{-1}$, which is consistent with $2.61 \times 10^{-8}\,m^4\,J^{-1}\,s^{-1}$ that extracted from the same GB based on the IRWalk method. This is strong indication that the existing MD methods that were developed based on pure systems can be applied to extract physical mobilities of GB with impurity segregation.

3.4. GB Diffusion of segregated dopants

Since it has been proposed in the CLS theory that the mobility of a migrating impure boundary is controlled by the impurity diffusion [10,11,20], we systematically investigated the diffusional behavior of segregated dopant atoms in the Al–Ni system. Specifically, the dopant diffusivity was extracted by using the Einstein relation $D^x_{dopant} = \langle x^2 \rangle / 2t$ for diffusion along x direction (parallel to the GB) and $D^z_{Dopant} = \langle z^2 \rangle / 2t$ for diffusion along the z direction (perpendicular to the GB) [33]. At each dopant concentration, we analyzed the evolution of the mean square displacement (MSD) of the dopants and the corresponding dopant diffusivity in two different ways: the results in Fig. 5(a–c) were based on the absolute movements of individual dopant atoms and the results in Fig. 6(a–c) were based on movements of individual dopant atoms relative to their COM, or in other words, in the reference of the moving GB according to Fig. 2(a and b). Specifically, Figs. 5(a) and 6(a) showed the evolution of absolute and relative MSD of Ni atoms along z direction (MSD^z) in Al–Ni system containing 5 Ni atoms at the GB. While a general linear trend was found between the MSD^z and t as predicted by the Einstein relation in both Figs. 5(a) and 6(a), it was surprising to see the significant variance among the 20 independent simulations. Although such variance was similar to that in Fig. 2(c and d), it was not caused by the thermal fluctuation of the GB because in Fig. 6(a) the variance was reduced but not completely cancelled out by eliminating the overall drift of the Ni atoms along with the GB plane. In the past, it was not uncommon to extract the dopant diffusivity in MD [33] by applying the Einstein relation based on only one single simulation, which could be considerably inaccurate by sampling only a small

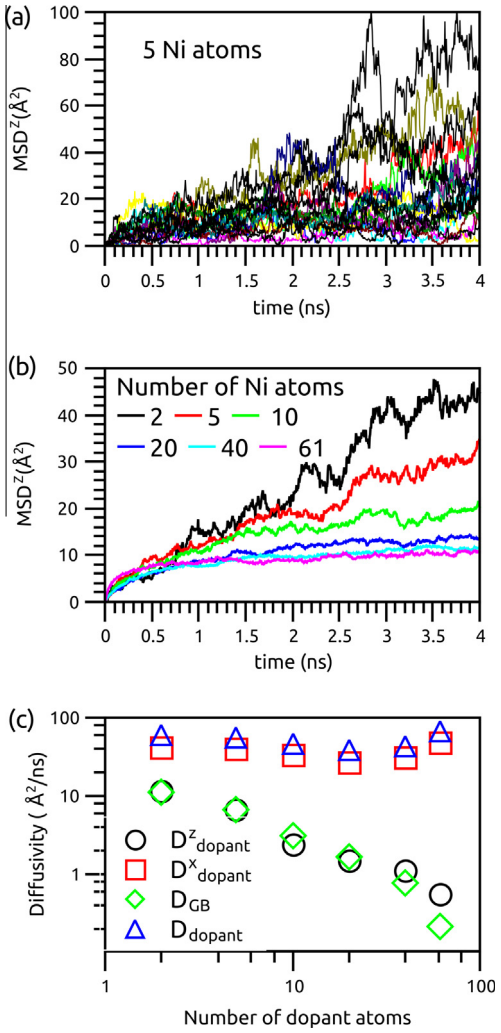

Fig. 5. (a) The evolution of the absolute MSD of impurities perpendicular to the GB plane in Al–Ni containing 5 Ni atoms. (b) The average of absolute MSD of dopant atoms as a function of the number of dopant atoms among 20 independent simulations. (c) The absolute diffusivity of the dopant atoms as a function of the number of dopant atoms. In (c), the superscripts x and z denote the directions parallel and perpendicular to the GB, subscript "dopant" denotes absolute dopant diffusivity. Solid lines are added as guide to the eye in (c). D_{GB} is the parameter used in Eq. (1).

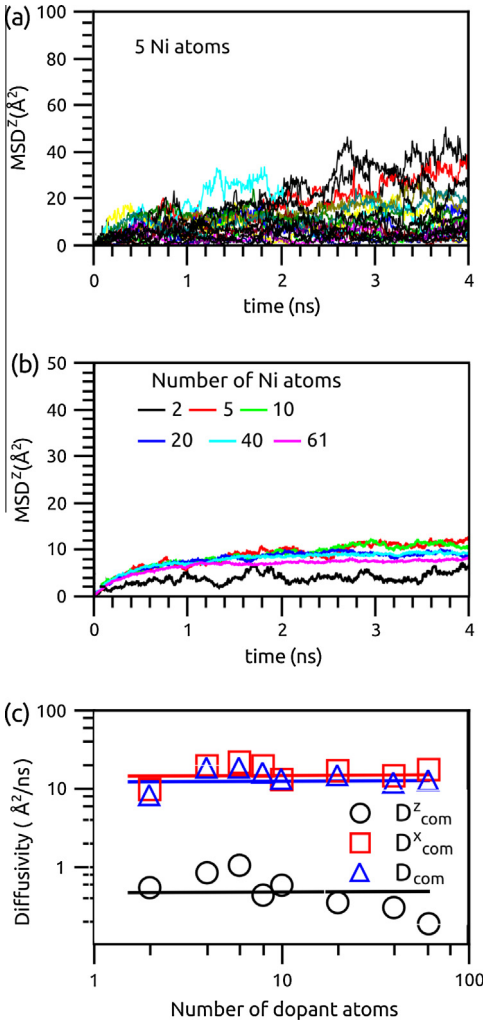

Fig. 6. (a) The evolution of the MSD of impurities relative to the COM of the impurity atoms perpendicular to the GB in Al–Ni containing 5 Ni atoms. (b) The average of MSD relative to the COM of dopant atoms as a function of the number of dopant atoms among 20 independent simulations. (c) The diffusivity of the dopant atoms relative to the COM as a function of the number of dopant atoms. In (c), the superscripts x and z denote the directions parallel and perpendicular to the GB, subscript "dopant" denotes absolute dopant diffusivity and "COM" denotes dopant diffusivity relative to their COM. Solid lines are added as guide to the eye in (c).

portion of the possible behaviors of the dopant atoms as indicated by Figs. 5(a) and 6(a).

Furthermore, it was found that the absolute dopant diffusivity perpendicular to the GB (D^z_{Dopant}) has a strong dependence on the solute concentration. As shown in Fig. 5(c), the slope of MSD^z *vs.* t decreased dramatically as the number of Ni atoms increased. Based on the Einstein relation, D^z_{Dopant} was extracted and plotted in Fig. 5(c), which showed exponential decrease as the dopant concentration increased. It is interesting to find that the "diffusion" coefficient D_{GB} used to extract the GB mobility M as defined in Eq. (1) was almost the same as D^z_{Dopant} (Fig. 5(c)). A strong correlation between the GB mobility M and the diffusivity of dopant atoms perpendicular to the GB D^z_{Dopant} can thus be established. In contrast, the diffusivity parallel to the GB (D^x_{Dopant}) remained relatively unchanged at all solute concentrations (Fig. 5(c)). Since the dopant diffusion parallel to the GB, e.g., along x and y direction was found to be similar and both significantly larger than that perpendicular to the GB (e.g., $D^x_{Dopant} \approx D^y_{Dopant} \gg D^z_{Dopant}$), the overall GB diffusivity of Ni atoms ($D_{Dopant} = \langle x^2 + y^2 + z^2\rangle/6t$) also remained relatively unchanged at different solute concentrations (Fig. 5(c)). However, by eliminating the overall drift of Ni atoms along with the GB and extracting the diffusivity of Ni atoms relative to their COM (Fig. 6(b and c)), the strong dependence of dopant diffusivity perpendicular to the GB on concentration no longer existed. For example, D^z_{com}, D^z_{com} and D^z_{com}, which denote the diffusivity of Ni atoms relative to their COM in the direction perpendicular to the GB, parallel to the GB, and the overall GB diffusivity, all showed weak or none dependence on the concentration (Fig. 6(c)).

3.5. Validation and modification of the CLS solute drag model

With the GB mobility and solute diffusivity extracted from direct MD simulations, it is now possible to quantitatively validate the CLS model. As suggested by Mendelev et al. [10,20,32], the mobility of an impure GB based on the CLS model can be expressed as

$$M = \frac{1}{1/M^0 + 1/M^{iimp}}, \quad M^{imp} = \frac{D}{2n\delta}\frac{1}{C_\infty}\frac{E^0}{(kT)^2}\left[\sinh\left(\frac{E^0}{kT}\right) - \frac{E^0}{kT}\right]^{-1} \tag{3}$$

where M^0 is the GB mobility in pure system, n is the number of dopant atoms per unit volume of the GB, δ is the GB thickness, E^0 is the heat of segregation for impurity, C_∞ is the bulk dopant concentration, and D is the bulk diffusion coefficient of the dopant. When there was no impurity, however, the GB in our model moved considerably faster than those with dopants which made it difficult to extract M^0 at the given temperature of 850 K. For example, at some initial conditions the GB could even move out of the model within as short as 1 ns. Therefore, it is reasonable to assume that M^0 is so large that the GB mobility M would be dominated by M^{imp} according to Eq. (3). The other parameters in Eq. (3) were obtained by the following steps.

We used a similar method as in Ref. [32] to determine the segregation energy E^0. First we let the model containing 10 dopant atoms in the GB fully relaxed at 850 K and zero pressure under NPT, then the temperature was reduced to 0 K in a stepwise fashion with the step of 50 K and 0.1 ns relaxation for each step under NPT. The same procedure was then performed on the same model, but the 10 dopant atoms were randomly placed in the bulk instead of in the GB. The difference of energy for those two models at $T = 0$ K divided by the number of impurity atoms is the segregation energy E^0. For Ni segregation in Al for the inclined $\Sigma5$ GB considered in this study, this energy was found to be −0.446 eV/atom. We have also applied this method to extract the segregation energy for Ti in Al, which was found to be 0.05 eV/atom. The positive segregation energy in Al–Ti system indicates that Ti atoms would rather remain in the bulk than segregate to the GB region. This trend is consistent with the observations in Fig. 1(d) that the Ti atoms would break away from the GB during the thermal fluctuation.

On the other hand, C_∞ is the bulk dopant concentration which correlates with the dopant concentration segregated at the GB C_0 [20,32] according to:

$$C_0 = C_\infty e^{-\frac{E^0}{kT}} \tag{4}$$

where E^0 is the same heat of segregation for impurity as in Eq. (3). In simulations performed in this study, we have assumed zero bulk concentration with all dopant atoms segregated to the GB. However, Eq. (4) can be used to estimate C_∞ that may lead to the same C_0 as studied in this research.

According to the original CLS model, D in Eq. (3) is the bulk diffusivity of dopant atoms. It was found that the bulk diffusion of Ni in Al obeyed the Arrhenius equation [34]:

$$D = Ae^{-\frac{Q}{kT}} \tag{5}$$

A is a frequency factor and Q is the activation energy. For Al–Ni system, $A = 4.4 \times 10^{-4}$ m^2 s^{-1}, $Q = -145.8$ kJ mol^{-1} [34]. Since the applicable temperature range for this value [34] is 742–924 K, it is appropriate for us to use this equation in estimating the bulk diffusion coefficient of Ni in Al system, which is 4.79×10^{-13} m^2 s^{-1}. It is very important to mention that the bulk diffusivity from the potential used in this study [26], which can be determined only through Monte Carlo simulations, would not be the same as the experimental value. However, since the bulk and GB diffusivity normally differ by several orders of magnitude, the experimental value (4.79×10^{-13} m^2 s^{-1}) is considered to be reasonable as compared to the GB diffusivity predicted by the interatomic potential [26] as shown in Fig. 6 (e.g., $D^z_{COM} \approx 5 \times 10^{-12}$ m^2 s^{-1}, $D_{COM} \approx 1.5 \times 10^{-10}$ m^2 s^{-1}).

The results by fitting Eq. (2) with the bulk diffusivity of Ni in Al system (4.79×10^{-13} m^2 s^{-1}) were shown in Fig. 7 with green diamond (denoted as *CLS1*). It can be seen that the fitted results were significantly smaller than those from the direct MD simulation (solid black circle). Nevertheless, the slopes of both trend lines were more or less the same. Since Fig. 5(c) suggested that the GB mobility mostly correlated to the solute diffusion perpendicular to the GB plane, the discrepancy between our simulation results and the fitting from Eq. (2) may stem from the use of bulk diffusivity of Ni in Al for D. Therefore, we fitted Eq. (2) again by replacing D with D^z_{Dopant} while other parameters remained the same; the results were shown in Fig. 7 with blue[1] triangle (denoted as *CLS2*). However, although the newly fitted results became closer to the simulation results in magnitude, the trend lines now differed significantly in slope.

Mendelev et al. have mentioned that Eq. (3) is a correction to the Einstein equation, which is derived in the frame of the moving boundary and could only be used in zero boundary velocity limit [10,20,32]. Therefore, D in Eq. (3) should not be the absolute diffusivity D^z_{Dopant} (Fig. 6(c)) but the relative diffusivity in the frame of the moving GB. Since the COM of dopant atoms always moved along with the GB in Al–Ni as shown in Fig. 2(c and d), the diffusivity of Ni in the frame of the moving GB would be perfectly approximated by the relative diffusion coefficient D^z_{com} as shown in Fig. 6(c). Also, based on John Cahn's model [20], δ is not the total GB thickness but half of it. Further corrections to the CLS model can thus be made by replacing D^z_{Dopant} in *CLS2* by D^z_{com}. Here the average of D^z_{com} at different concentrations shown in Fig. 6(c) was used to fit Eq. (3). The newly fitted results based on D^z_{com} were

[1] For interpretation of color in Fig. 7, the reader is referred to the web version of this article.

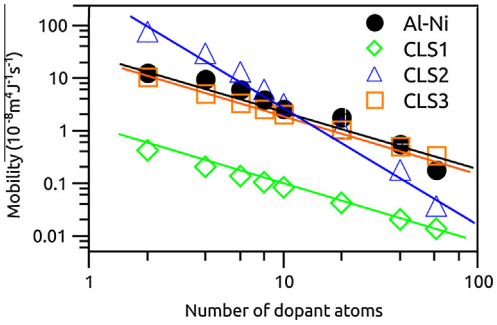

Fig. 7. Theoretical predictions based on CLS model by using bulk diffusivity D (*CLS1*), D^{z}_{Dopant} (*CLS2*) and D^{z}_{com} (*CLS3*) in Al–Ni system. Solid lines are added as guide to the eye.

denoted as *CLS3* in Fig. 5(c) with orange squares, which closely matched the MD simulation results in both the slope and magnitude. It needs to be mentioned, however, the modification to the original CLS model by using a different diffusivity in Eq. (3) needs to be validated by more data, for example, extracted at different temperatures or in different alloying systems, which warrants further study. Nevertheless, the excellent agreement between MD simulations and analytical modeling shown in Fig. 7 should shed important light on the understanding of the fundamental mechanisms of solute drag effects in GB networks.

4. Conclusions

In summary, we quantified the GB mobility with impurities by direct MD simulations and validated the solute-drag based CLS theory. In particular, the following three main conclusions can be drawn from this research:

- Existing MD methods for studying pure GB systems can be readily extended to investigate impure GB systems and extract physical mobilities under experimental conditions.
- The main assumption in the CLS solute drag theory was confirmed that the migration of impure GB was indeed controlled by dopant diffusion, but the dopant diffusion in the direction perpendicular to the GB ultimately determined the GB mobility.
- A correction to the original CLS model was proposed by replacing the impurity bulk diffusivity by the impurity diffusivity perpendicular to the GB plane in the frame of the moving GB so that the MD simulations results can perfectly match the predictions from the theoretical CLS model.

Acknowledgements

This work was supported by the University of Manitoba Graduate Fellowship (UMGF) and enabled by the use of computing resources provided by WestGrid and Compute/Calcul Canada.

References

[1] A.J. Detor, C.A. Schuh, J. Mater. Res. 22 (2011) 3233–3248, http://dx.doi.org/10.1557/JMR.2007.0403.
[2] G. Gottstein, L.S. Shvindlerman, Grain Boundary Migration in Metals, 2nd ed., CRC Press, Taylor & Francis Group, Boca Raton, 2010.
[3] C.E. Krill III, L. Helfen, D. Michels, H. Natter, A. Fitch, O. Masson, et al., Phys. Rev. Lett. 86 (2001) 842.
[4] J.C. Li, Phys. Rev. Lett. 96 (2006) 215506.
[5] H.J. Fecht, Phys. Rev. Lett. 65 (1990) 610.
[6] T. Chookajorn, H.A. Murdoch, C.A. Schuh, Science 337 (2012) 951–954, http://dx.doi.org/10.1126/science.1224737.
[7] J. Trelewicz, C. Schuh, Phys. Rev. B. 79 (2009), http://dx.doi.org/10.1103/PhysRevB.79.094112.
[8] P.C. Millett, R.P. Selvam, A. Saxena, Acta Mater. 55 (2007) 2329–2336, http://dx.doi.org/10.1016/j.actamat.2006.11.028.
[9] P.C. Millett, R.P. Selvam, A. Saxena, Acta Mater. 54 (2006) 297–303, http://dx.doi.org/10.1016/j.actamat.2005.07.024.
[10] J.W. Cahn, Acta Metall. 10 (1962) 789–798, http://dx.doi.org/10.1016/0001-6160(62)90092-5.
[11] K. Lücke, H.P. Stüwe, Acta Metall. 19 (1971) 1087–1099.
[12] K. Lücke, K. Detert, Acta Metall. 5 (1957) 628–637, http://dx.doi.org/10.1016/0001-6160(57)90109-8.
[13] K.G.F. Janssens, D. Olmsted, E.A. Holm, S.M. Foiles, S.J. Plimpton, P.M. Derlet, Nat. Mater. 5 (2006) 124–127, http://dx.doi.org/10.1038/nmat1559.
[14] D.L. Olmsted, E.A. Holm, S.M. Foiles, Acta Mater. 57 (2009) 3704–3713, http://dx.doi.org/10.1016/j.actamat.2009.04.015.
[15] H. Zhang, M.I. Mendelev, D.J. Srolovitz, Acta Mater. 52 (2004) 2569–2576, http://dx.doi.org/10.1016/j.actamat.2004.02.005.
[16] H. Zhang, D. Du, D.J. Srolovitz, Philos. Mag. 88 (2008) 243–256, http://dx.doi.org/10.1080/14786430701810764.
[17] Z.T. Trautt, M. Upmanyu, A. Karma, Science 314 (2006) 632–635, http://dx.doi.org/10.1126/science.1131988.
[18] P.C. Millett, R.P. Selvam, S. Bansal, A. Saxena, Acta Mater. 53 (2005) 3671–3678, http://dx.doi.org/10.1016/j.actamat.2005.04.031.
[19] A. Suzuki, Y. Mishin, Atomistic modeling of point defects and diffusion in copper grain boundaries, INTERFACE Sci. (2003) 131–148.
[20] M.I. Mendelev, D.J. Srolovitz, Model. Simul. Mater. Sci. Eng. 10 (2002) R79–R109, http://dx.doi.org/10.1088/0965-0393/10/6/201.
[21] M.I. Mendelev, D.J. Srolovitz, Acta Mater. 49 (2001) 589–597, http://dx.doi.org/10.1016/S1359-6454(00)00358-X.
[22] C. Deng, C.A. Schuh, Phys. Rev. Lett. 106 (2011), http://dx.doi.org/10.1103/PhysRevLett. 106.045503.
[23] C. Deng, C.A. Schuh, Phys. Rev. B. 84 (2011), http://dx.doi.org/10.1103/PhysRevB.84.214102.
[24] M.I. Mendelev, C. Deng, C.A. Schuh, D.J. Srolovitz, Model. Simul. Mater. Sci. Eng. 21 (2013) 045017, http://dx.doi.org/10.1088/0965-0393/21/4/045017.
[25] S. Plimpton, J. Comput. Phys. 117 (1995) 1–19, http://dx.doi.org/10.1006/jcph.1995.1039.
[26] G.P. Purja Pun, Y. Mishin, Philos. Mag. 89 (2009) 3245–3267.
[27] A. Landa, P. Wynblatt, D.J. Siegel, J.B. Adams, O.N. Mryasov, X.-Y. Liu, Acta Mater. 48 (2000) 1753–1761, http://dx.doi.org/10.1016/S1359-6454(00)00002-1.
[28] R.R. Zope, Y. Mishin, Phys. Rev. B. 68 (2003) 024102.
[29] J. Li, Model. Simul. Mater. Sci. Eng. 11 (2003) 173.
[30] X. Xie, Y. Mishin, Acta Mater. 50 (2002) 4303–4313, http://dx.doi.org/10.1016/S1359-6454(02)00262-8.
[31] M.I. Mendelev, D.J. Srolovitz, Acta Mater. 49 (2001) 2843–2852, http://dx.doi.org/10.1016/S1359-6454(01)00175-6.
[32] M.I. Mendelev, D.J. Srolovitz, G.J. Ackland, S. Han, J. Mater. Res. 20 (2011) 208–218, http://dx.doi.org/10.1557/JMR.2005.0024.
[33] T. Frolov, S.V. Divinski, M. Asta, Y. Mishin, Phys. Rev. Lett. 110 (2013), http://dx.doi.org/10.1103/PhysRevLett. 110.255502.
[34] E.A. Brandes, G.B. Brook (Eds.), Smithells Metals Reference Book, 7th ed., Butterworth-Heinemann, Oxford, Boston, 1998.